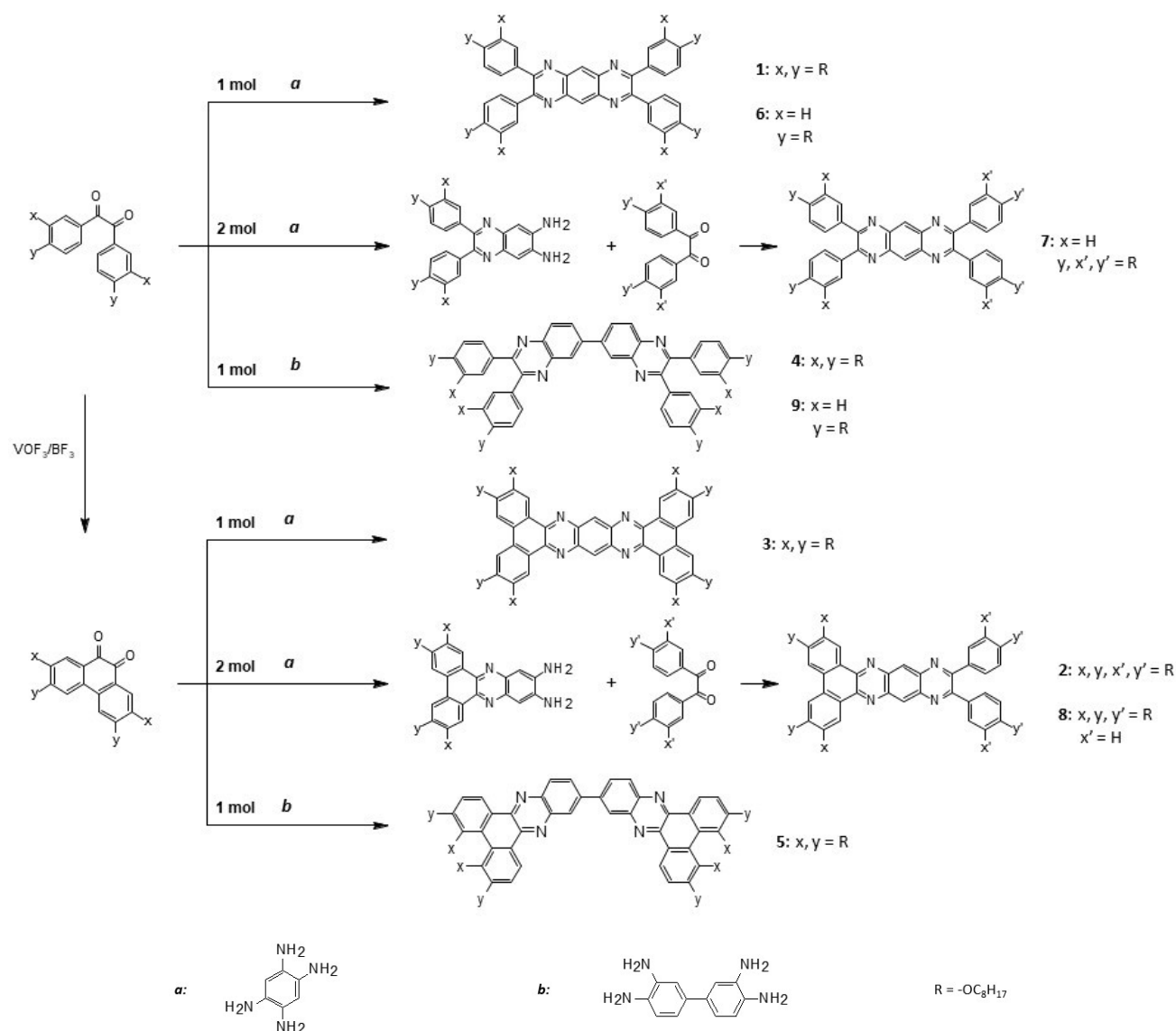


## Chiral columns forming lattice with giant unit cell

Paulina Rybak\*, Adam Krowczynski, Jadwiga Szydłowska, Damian Pocięcha and Ewa Gorecka

### Synthesis



**Scheme S1.** Schematic representation of the synthesis of obtained compounds.

Preparation of compounds: **1**, **6** and **7** followed the prescription given by Walsh<sup>1</sup>, Wang<sup>2</sup> and Vishwakarma<sup>3</sup>. Phenantrenequinone was prepared after Mohr<sup>4</sup>. After coupling the same procedure as in abovementioned prescriptions was followed to obtain compounds **3**, **2** and **8**; The intermediate product (coupled and uncoupled diamines) in synthesis of **7**, **2** and **8** was prepared according to the prescription described by Krzyczkowska et al.<sup>5</sup>.

Synthesis with **b** of compounds: **4**, **5** and **9** was performed in the same conditions as in the case of **a**; solvents used for dibenzoylation to the amines were acetic acid and isopropanol.

**NMR, mass spectra and elemental analysis:**

<sup>1</sup>H and <sup>13</sup>C NMR spectra were recorded on Agilent 400 MHz and Bruker 500 MHz NMR spectrometers. Mass spectroscopy was conducted on Micromass LCT.

**Compound 1.** pyrazino[2,3-g]quinoxaline, 2,3,7,8-tetrakis[3,4-bis(octyloxy)phenyl]:

<sup>1</sup>H NMR (400 MHz, CDCl<sub>3</sub>): δ = 0.82-1.87 (m, 120 H); 3.86 (t, J=6.7 Hz, 8 H); 4.02 (t, J=6.7 Hz, 8 H); 6.86 (d, J= 8.3 Hz, 4 H); 7.15 (d, J=2.0 Hz, 4 H); 7.2 (dd, J=2.0 Hz, 8.3 Hz, 4 H); 8.89 (s, 2 H)

<sup>13</sup>C NMR (400 MHz, CDCl<sub>3</sub>): δ = 154.68; 150.31; 148.68; 140.18; 131.53; 127.89; 123.09; 115.30; 113.00; 69.19; 69.16; 31.84; 31.83; 29.40; 29.37; 29.33; 29.28; 29.20; 29.13; 29.02; 26.02; 22.69; 22.67; 14.09

HRMS exact mass calculated for C<sub>98</sub>H<sub>150</sub>N<sub>4</sub>O<sub>8</sub>: 1512.2616; found: 1512.0453

Elemental analysis (%) calculated: C 77.83, H 10.00, N 3.71; Found: C 77.65, H 9.97, N 3.64

**Compound 2** [2,3,6,7]-tetra-(octyloxy)-[12,13]-(di-([3,4]-di-octyloxy)-phenyl)-[9,11,14,16]-tetraaza-tetracene:

<sup>1</sup>H NMR (400 MHz, CDCl<sub>3</sub>): δ = 0.87-2.04 (m, 120 H); 3.88 (t, J=6.7 Hz, 4 H); 4.04 (t, J=6.7 Hz, 4H); 4.28 (t, J=6.6 Hz, 4 H); 4.37 (t, J=6.6 Hz, 4 H); 6.88 (d, J=8.5 Hz, 2 H); 7.19 (d, J=2.0 Hz, 2 H); 7.2 (dd, J=2.0 Hz, 8.5 Hz, 2 H); 7.67 (s, 2 H); 8.82 (s, 2 H); 9.1 (s, 2 H)

<sup>13</sup>C NMR (400 MHz, CDCl<sub>3</sub>): δ = 154.40; 152.35; 150.29; 149.42; 148.67; 143.76; 140.75; 139.66; 131.73; 127.58; 127.12; 123.61; 123.16; 115.34; 112.93; 109.40; 106.52; 69.47; 69.19; 31.88; 31.85; 31.84; 29.48; 29.42; 29.39; 29.36; 29.34; 29.33; 29.31; 29.29; 29.23; 29.17; 26.19; 26.15; 26.04; 22.71; 22.69; 22.67; 14.10

HRMS exact mass calculated for C<sub>98</sub>H<sub>148</sub>N<sub>4</sub>O<sub>8</sub>: 1510.2457; found: 1510.2963

Elemental analysis (%) calculated: C 77.95, H 9.88, N 3.71; Found: C 78.04, H 9.89, N 3.62

**Compound 3** [2,3,6,7,13,14,17,18]-octa-(octyloxy)-tetrabenzo-[a,c,l,n]-[9,11,20,22]-tetraaza-pentacene:

<sup>1</sup>H NMR (500 MHz, CDCl<sub>3</sub>, 50°C): δ = 0.92-2.03 (m, 120 H); 4.18 (t, J=6.6 Hz, 8 H); 4.30 (t, J=6.6 Hz, 8 H); 7.45 (s, 4 H); 8.63 (s, 4 H); 8.96 (s, 4 H)

<sup>13</sup>C NMR (500 MHz, CDCl<sub>3</sub>, 50°C): δ = 152.23; 149.45; 143.36; 140.02; 126.94; 123.9; 109.64; 106.72; 69.61; 69.17; 31.99; 31.95; 29.68; 29.63; 29.44; 29.42; 26.36; 26.31; 22.76; 22.73; 14.10; 14.07

HRMS exact mass calculated for C<sub>98</sub>H<sub>146</sub>N<sub>4</sub>O<sub>8</sub>: 1508.2298; found: 1508.2406

Elemental analysis (%) calculated: C 78.04, H 9.76, N 3.71; Found: C 77.95, H 9.77, N 3.66

**Compound 4** 2,3,2',3'-tetrakis-(3,4-bis-octyloxy-phenyl)-[6,6']biquinoxaline:

<sup>1</sup>H NMR (400 MHz, CDCl<sub>3</sub>): δ = 0.84-1.87 (m, 120 H); 3.82-3.88 (m, 8 H); 4.01 (broad t, J=6.7 Hz, 8 H); 6.85 (broad d, J=8.4 Hz, 4 H); 7.1 (d, J=2.1 Hz, 2 H); 7.12 (d, J= 2.1 Hz, 2 H); 7.13-7.17 (m, 4 H); 8.18 (dd, J=1.9 Hz, 8.7 Hz, 2 H); 8.25 (d, J=8.7 Hz, 2 H); 8.54 (d, J=1.9 Hz, 2 H)

<sup>13</sup>C NMR (400 MHz, CDCl<sub>3</sub>): δ = 153.79; 153.37; 149.94; 148.70; 141.20; 140.82; 140.66; 131.71; 131.69; 129.63; 128.99; 127.16; 122.85; 115.30; 115.28; 113.16; 113.12; 69.16; 31.84; 31.83; 29.41; 29.38; 29.33; 29.28; 29.23; 29.15; 26.03; 22.69; 22.67; 14.09

HRMS exact mass calculated for C<sub>104</sub>H<sub>154</sub>N<sub>4</sub>O<sub>8</sub>: 1588.3576; found: 1588.3443

Elemental analysis (%) calculated: C 78.64, H 9.77, N 3.53; Found: C 78.65, H 9.67, N 3.38

**Compound 5** 11,11'-bi(di-[2,3,6,7,2',3',6',7']-octa-(octyloxy)-benzo)-[a,c]-phenazine:

<sup>1</sup>H NMR (500 MHz, CDCl<sub>3</sub>, 50°C): δ = 0.89-1.99 (m, 120 H); 4.24-4.27 (m, 8 H); 4.31-4.36 (m, 8 H); 7.63 (s, 2 H); 7.64 (s, 2 H); 8.29 (dd, J=2.0 Hz, 8.8 Hz, 2 H); 8.37 (d, J=8.8 Hz, 2 H); 8.72 (broad s, 4 H)

<sup>13</sup>C NMR (500 MHz, CDCl<sub>3</sub>, 50°C): δ = 151.93; 149.58; 142.38; 141.96; 141.74; 141.27; 140.25; 129.75; 128.48; 127.33; 126.64; 126.60; 124.01; 123.88; 109.12; 109.07; 106.80; 106.73; 69.79; 69.25; 31.96; 31.94; 29.63; 29.60; 29.57; 29.56; 29.42; 29.41; 26.36; 26.33; 26.30; 22.75; 22.73; 14.10; 14.08

HRMS exact mass calculated for C<sub>72</sub>H<sub>90</sub>N<sub>4</sub>O<sub>4</sub>: 1075.5094; found: 1076.0352

Elemental analysis (%) calculated: C 80.41, H 8.43, N 5.21; Found: C 79.65, H 8.37, N 5.24

**Compound 6** pyrazino[2,3-g]quinoxaline, 2,3,7,8-tetrakis[4-(octyloxy)phenyl]:

<sup>1</sup>H NMR (400 MHz, CDCl<sub>3</sub>): δ = 0.88-1.84 (m, 60 H); 4.0 (t, J=6.6 Hz, 8 H); 6.89 and 7.58 (AA', BB', J=8.8 Hz, 16 H); 8.87 (s, 2H)

<sup>13</sup>C NMR (400 MHz, CDCl<sub>3</sub>): δ = 160.20; 154.51; 140.21; 131.44; 131.27; 127.86; 114.30; 68.10; 31.82; 29.37; 29.24; 29.22; 26.04; 22.66; 14.11

HRMS exact mass calculated for C<sub>66</sub>H<sub>86</sub>N<sub>4</sub>O<sub>4</sub>: 999.4134; found: 999.4204

Elemental analysis (%) calculated: C 79.32, H 8.67, N 5.61; Found: C 79.65, H 8.72, N 5.56

**Compound 7** pyrazine [2,3-g]quinoxaline, 2,3-di[3,4-bis(octyloxy)phenyl], 7,8-di[4-(octyloxy)phenyl]:

<sup>1</sup>H NMR (400 MHz, CDCl<sub>3</sub>): δ = 0.87-1.87 (m, 90 H); 3.86 (t, J=6.7 Hz, 4 H); 4.0 (t, J=6.6 Hz, 4H); 4.02 (t, J=6.6 Hz, 4 H); 6.87 (d, J=8.3 Hz, 2 H); 7.89 and 7.58 (AA', BB', J=8.8 Hz, 8 H); 7.15 (d, J=2.0 Hz, 2 H); 7.21 (dd, J=2.1 Hz, 8.3 Hz, 2 H); 8.88 (s, 2 H)

<sup>13</sup>C NMR (400 MHz, CDCl<sub>3</sub>): δ = 160.22; 154.65; 154.58; 150.30; 148.68; 140.25; 140.15; 132.19; 131.55; 131.43; 131.25; 127.88; 123.08; 121.61; 115.31; 114.32; 114.04; 113.88; 113.02; 69.20; 29.17; 68.22; 68.11; 31.85; 31.83; 31.81; 29.40; 29.37; 29.36; 29.33; 29.31; 29.28; 29.23; 29.21; 29.13; 26.03; 22.69; 22.67; 22.65; 14.09

HRMS exact mass calculated for C<sub>82</sub>H<sub>118</sub>N<sub>4</sub>O<sub>6</sub>: 1255.8375; found: 1256.0212

Elemental analysis (%) calculated: C 78.42, H 9.47, N 4.46; Found: C 78.54, H 9.52, N 4.53

**Compound 8** [2,3,6,7]-tetraoctyloxy-12,13-di(4'-octyloxyphenyl)-dibenzo[a,c]-9,11,14,16-tetraazatetracene:

<sup>1</sup>H NMR (400 MHz, CDCl<sub>3</sub>): δ = 0.87-2.03 (m, 90 H); 4.01 (t, J=6.6 Hz, 4 H); 4.22 (t, J=6.6 Hz, 4 H); 4.35 (t, J=6.6 Hz, 4 H); 6.9 and 7.59 (AA', BB', J=8.8 Hz, 8 H); 7.57 (s, 2 H); 8.73 (s, 2H); 9.01 (s, 2 H)

<sup>13</sup>C NMR (400 MHz, CDCl<sub>3</sub>): δ = 160.10; 153.97; 152.07; 149.13; 143.38; 140.50; 139.52; 131.52; 131.49; 127.39; 126.78; 123.34; 114.15; 109.13; 105.96; 69.29; 69.01; 68.09; 31.95; 31.91; 31.85; 29.63; 29.59; 29.44; 29.42; 29.40; 29.28; 26.28; 26.20; 26.09; 22.76; 22.73; 22.68; 14.16; 14.13; 14.12

HRMS exact mass calculated for C<sub>82</sub>H<sub>116</sub>N<sub>4</sub>O<sub>6</sub>: 1253.8216; found: 1253.7984

Elemental analysis (%) calculated: C 78.55, H 9.33, N 4.47; Found: C 78.65, H 9.27, N 4.36

**Compound 9** 2,3,2',3'-tetrakis-(4-octyloxy-phenyl)-[6,6']-biquinoxaline:

<sup>1</sup>H NMR (400 MHz, CDCl<sub>3</sub>): δ = 0.86-1.83 (m, 60 H); 3.98 (broad t, J=6.6 Hz, 8 H); 6.88 and 7.52 (broad AA', BB', J=8.8 Hz, 16 H); 8.15 (dd, J=2.0 Hz, 8.8 Hz, 2 H); 8.23 (d, J=8.8, 2 H); 8.51 (d, J=2.0 Hz, 2 H)

<sup>13</sup>C NMR (400 MHz, CDCl<sub>3</sub>): δ = 159.85; 159.84; 153.69; 153.25; 141.25; 140.82; 140.71; 131.41; 131.40; 131.24; 129.62; 128.97; 127.14; 114.33; 68.08; 31.81; 29.37; 29.24; 29.23; 26.04; 22.66; 14.10

HRMS exact mass calculated for C<sub>72</sub>H<sub>90</sub>N<sub>4</sub>O<sub>4</sub>: 1075.5094; found: 1075.7056

Elemental analysis (%)calculated: C 80.41, H 8.43, N 5.21; Found: C 81.04, H 8.62, N 5.24

**Experimental****Calorimetry**

Calorimetric studies were performed with a TA DSC Q200 calorimeter, samples of mass from 1 to 3 mg were sealed in aluminium pans and kept in nitrogen atmosphere during measurement, and both heating and cooling scans were performed with a rate of 5–10 K/min.

**Microscopic studies**

Optical studies were performed by using the Zeiss Imager A2m polarizing microscope equipped with Linkam heating stage.

**X-Ray diffraction**

The X-ray diffraction patterns were obtained with the Bruker D8 GADDS system (CuKα line, Goebel mirror, point beam collimator, Vantec2000 area detector). Samples were prepared as droplets on a heated surface.

**Luminescence studies**

Absorption spectra were measured for diluted in methylene chloride solutions (concentration about 2-4·10<sup>-2</sup> g·dm<sup>-3</sup>) using spectrometer: Shimadzu PC3100. Emission spectra was detected using FluoroLog HORRIBA Jobin Ivon. Fluorescence quantum yields were measured using the standard method, with fluorescein dissolved in 0,1M NaOH as referential material.

$$\varphi = \varphi_{ref} \frac{Grad_x}{Grad_{ref}} \cdot \frac{n_{DCM}^2}{n_{NaOH}^2}$$

(fluorescein quantum yield:  $\varphi_{ref} = 0,79$ ; refractive indices:  $n_{DCM} = 1,424$ ;  $n_{NaOH} = 1,335$ )

**Charge mobility**

The TOF experiments were performed in a conventional setup. The 10 μm thick cell was used with ITO electrodes covered with homogeneously aligning surfactant, the cells were filled using capillary forces, the applied voltage was in the range of 11–117 V. The transient photocurrent was measured over 5 kΩ and 100 kΩ (form electron current) resistor and recorded with 300 MHz digitizing oscilloscope (Agilent Technologies DSO6034A) triggered by the laser pulse. The estimated response time of the whole setup was less than 2.5 μs. The charges (holes and electrons) were generated by a short light pulse (355 nm and 532 nm wavelengths, ≈8 ns pulse width) coming from a solid-state laser EKSPLA NL202. The sample was illuminated by a single pulse manually triggered to give the sample enough time for relaxation. To reduce a noise the data were collected over 16 runs and averaged. If the registered hole photocurrent curves were nondispersive the clear cutoff enabling precise determination the transient time, τ. The transient time τ was determined as the intersection of two lines tangential to the plateau and “current tail.” Form the transient time τ the charge (hole) mobility was calculated according to formula:  $\mu = d/(\tau E)$ , where d is the sample thickness (cm), E is the strength of electric field (V cm<sup>-1</sup>), and τ is the time of flight (τ/s).

**Electrochemistry**

In order to record electrochemical data we measured cyclic voltammetry (CV) and differential pulse voltammetry (DPV) using the bipotentiostat (CH Instruments 750E, Austin, Tx, USA) in registered in DCM solutions with tetrabutylammonium hexafluoro phosphate, also in DCM, as supporting electrolyte. Measurements were carried out in the three electrode arrangements, with calomel electrode as the reference electrode, platinum foil as the counter and glassy carbon electrode (GCE, BASi, A=0.070 cm<sup>2</sup>) as the working electrode. The analyzed samples were deoxygenated prior to measurements by purging with argon (99.999 %) for 20 min and then argon was passed over the solution surface. At each measurement series the reference electrode potential was calibrated using ferrocene (Fc/Fc<sup>+</sup>) in the same supporting electrolyte solution and the calibration constant  $E_{Ferr}$  were found. The values of the formal potentials,  $E_{1/2}$ , obtained for each redox step in the voltammograms.  $E_{1/2}$  was

approximated as  $(E_{pa} + E_{pc})/2$ , where  $E_{pa}$  and  $E_{pc}$  are the oxidation and reduction peak potentials, respectively. The formal potentials were determined from cyclic voltammetry waves as averaged oxidation/reduction potential. When CV waves were not clearly shaped the square wave voltammetry was applied. The energies of HOMO/LUMO levels of a given compound ( $E_{HOMO}$  and  $E_{LUMO}$ ) were evaluated from its first oxidation and the first reduction potentials. The energy  $E_{HOMO}$  and  $E_{LUMO}$  levels were calculated according to the following equations  $E_{HOMO} = -(E_{ox} - E_{ferr} + 4.8)$  eV and  $E_{LUMO} = -(E_{red} - E_{ferr} + 4.8)$  eV.

### Additional experimental results

The mesogenic compounds were shown and described in the main article. Here we present additional data regarding those mesogens along with other obtained compounds (Fig. S2), that did not exhibit any additional phases between crystallization and isotropic liquid but did give interesting spectral response. Among all obtained compounds, in order to exhibit liquid crystalline properties it is crucial to have two chains substituted in every single peripheral ring.

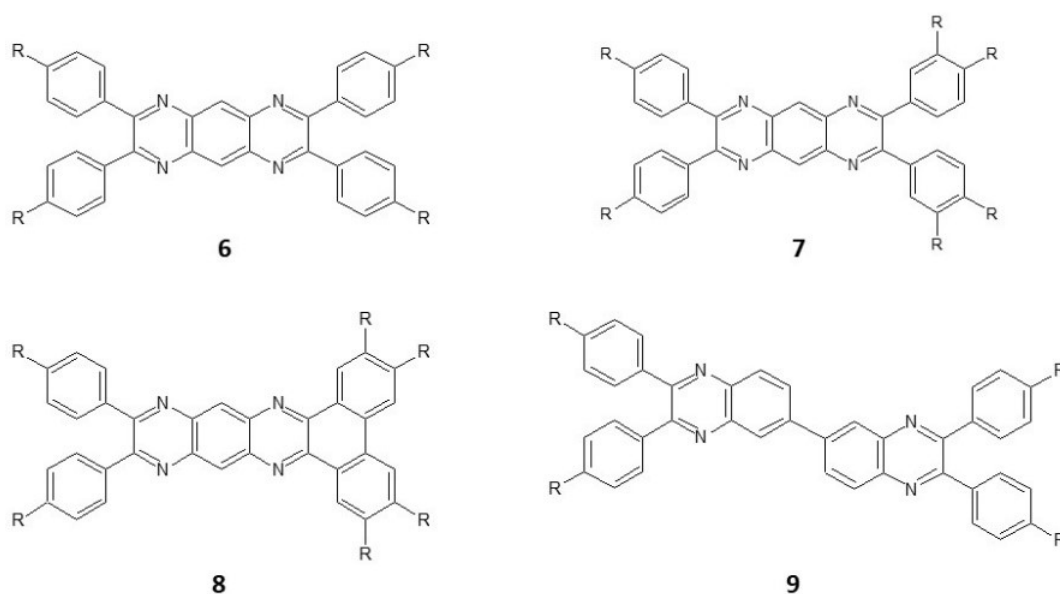


Figure S1. Non-liquid crystalline compounds, R =  $-\text{OC}_8\text{H}_{17}$

Table S1. Phase transition temperatures [ $^{\circ}\text{C}$ ] and associated thermal effects [J/g] (in parentheses) for obtained compounds;

Phase transition	
6	Cry - 192.8 (54.9) - Iso
7	Cry - 140.0 (42.2) - Iso
8	Cry - 164.1 (47.3) - Iso
9	Cry - 126.6 (35.8) - Iso

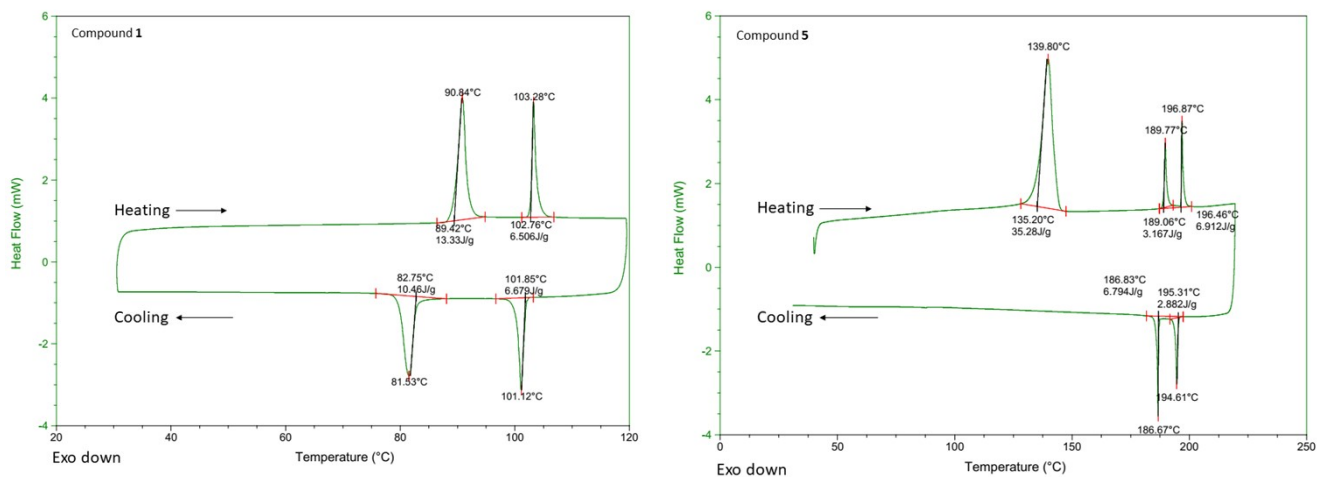


Figure S2. DSC plot of compound 1 and 5

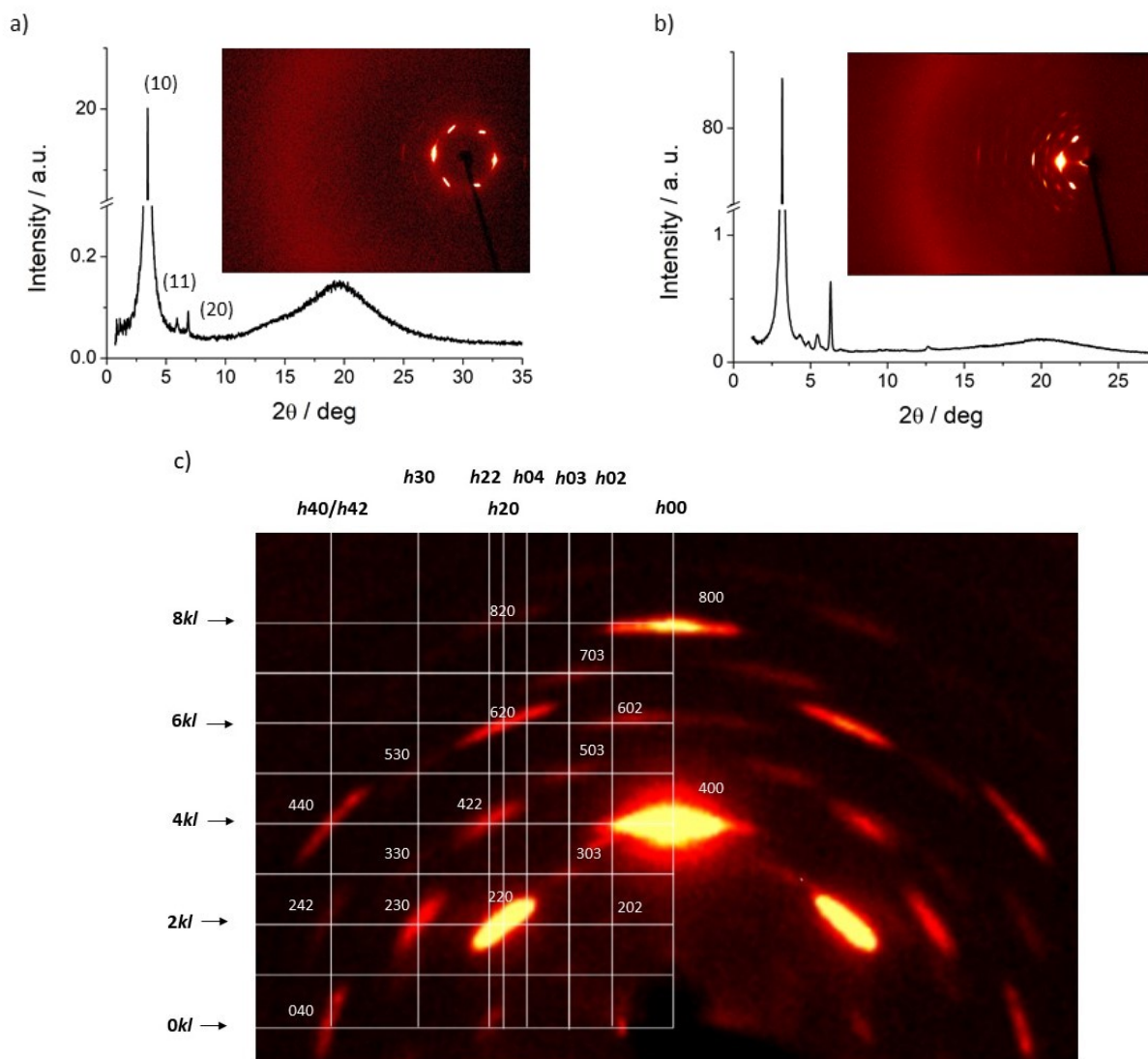


Figure S3. Wide angle XRD patterns for: (a)  $Col_h$  phase and (b)  $Col_{Fdd}$  phase of compound 1 at 102°C and 50°C, respectively; (c) small angle XRD pattern of  $Col_{Fdd}$  phase of compound 1 with superimposed reciprocal lattice.

**Table S2.** Experimental and calculated signal positions and crystallographic lattice parameters for compounds **1** and **5** in  $Col_{Fddd}$  phase; d values were using unit cell parameters: for compound **1**:  $a=113.11\text{\AA}$ ,  $b=65.31\text{\AA}$ ,  $c=155.42\text{\AA}$  and for compound **5**:  $a=107.63\text{\AA}$ ,  $b=62.14\text{\AA}$ ,  $c=49.75\text{\AA}$ .

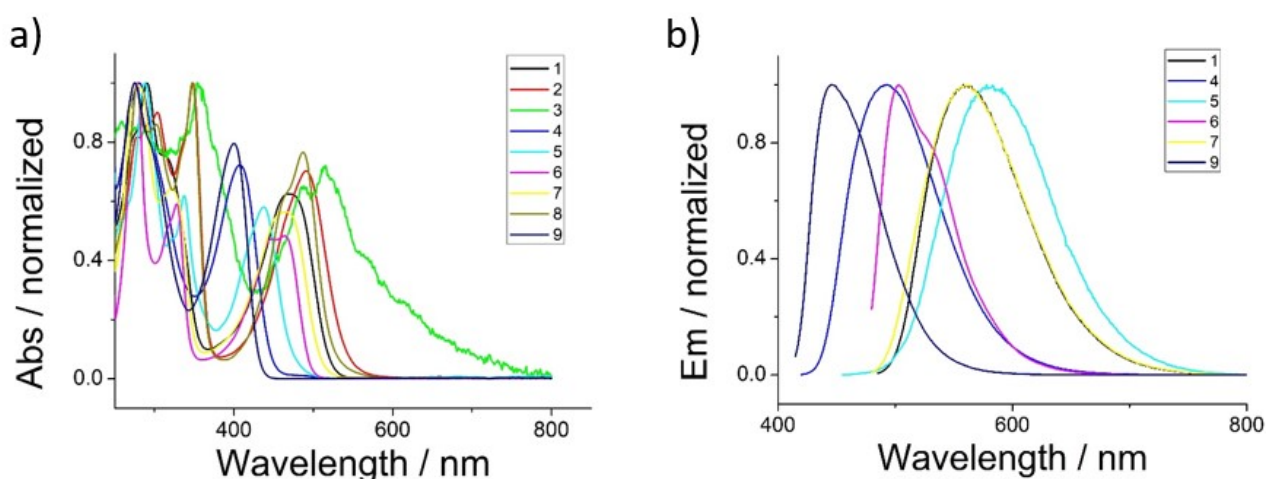
<b>Compound 1</b>			<b>Compound 5</b>		
$d_{exp}$	$d_{calc}$	$hkl$	$d_{exp}$	$d_{calc}$	$hkl$
45.66	45.73	202	27.06	26.91	220
30.44	31.95	303	26.90	26.91	400
30.31	30.10	022	26.58	26.35	311
28.14	28.28	220	19.16	18.83	131
28.32		400	18.82		511
22.74	22.86	224	17.04	16.88	331
23.04		404			
20.56	21.18	503	15.69	15.53	040
			15.59		620
20.33	20.61	422	14.36	14.30	531
			14.30		711
20.26	20.29	230	13.58	13.45	440
			13.45		800
19.42	19.76	513	12.13	12.00	151
18.72	18.01	331	12.03	11.98	731
18.36		317			
16.16	16.33	040	11.53	11.43	351
16.25		620	11.44		911
15.42	15.61	531	10.63	10.52	551
15.47		703			
15.37	15.38	242	10.25		260
			10.26	10.17	840
			10.15		10 20
14.06	14.14	440	9.55	9.49	751
14.11		800	9.46		11 11
13.26	12.93	731	9.02	8.97	660
			8.96		12 00
12.72	12.80	822	8.85	8.71	171
			8.73		11 31
12.23	12.31	824	8.16	8.10	571
12.22	12.30	911	7.54	7.46	480
11.12	11.19	10 02	7.87	7.77	080
			7.79		12 40
10.72	10.78	062	7.46	7.46	14 20
			7.50		10 60
10.11	10.15	6 2 12			
10.10	10.13	11 11			
10.11	10.07	462			
9.39	9.43	12 00			
8.94	8.99	12 22			

**Table S3.** Absorption and emission peaks, measured in DCM solutions;

	$\lambda_{exc}^6$	$\lambda_{em}^6$	Stokes shift <sup>6</sup>	$\phi_{solution}$	$\phi_{solid}$
6	462	502	40	0.36	0.65
7	465	543	78	0.05	0.35
8	486	-	-	-	-
9	400	446	46	0.4	0.11

Compounds **1-3** and **6-8** with the central part of the molecule built with pyrazino-quinoxaline structure, have absorption spectra red-shifted dependent on the extension of the  $\pi$ -conjugated system. Among **1-3** compounds the most red-shifted is mesogen **3**, with the most rigid central core (23 nm shift according to **1**). The same effect can be observed for compounds **4** and **5** (29 nm shift). The other factor that has the influence on the absorption spectra shift is the number of terminal alkoxy chains. This effect is visible comparing spectra of compounds **1** with **6** (25 nm shift), **2** with **8** (19 nm shift) and **4** with **9** (14 nm shift). Those are expected results due to the fact that free electron couple from oxygen can be included in the  $\pi$ -conjugated system. From this two factors bigger impact lays in the rigidity of the core.

When it comes to emission spectra, compounds (**2, 3** and **8**) with the highest rigidity of the pyrazino-quinoxaline core, where at least two peripheral phenyl rings are coupled, do not show spectral response to the excitation wave. As for the number of terminal chains its impact is not explicit, because compounds **1** and **7** with 8 and 6 alkoxy chains, respectively, have almost identical emission spectra, whereas compound **6**, with 4 alkoxy chains has spectra less red-shifted. For the compounds with the biphenyl-based core (**4, 5** and **9**) the most red-shifted emission spectra was detected for compound **5** with adjacent phenyl rings and 8 terminal chains.

**Figure S4.** Normalized absorption (a) and emission (b) spectra for all obtained compounds;

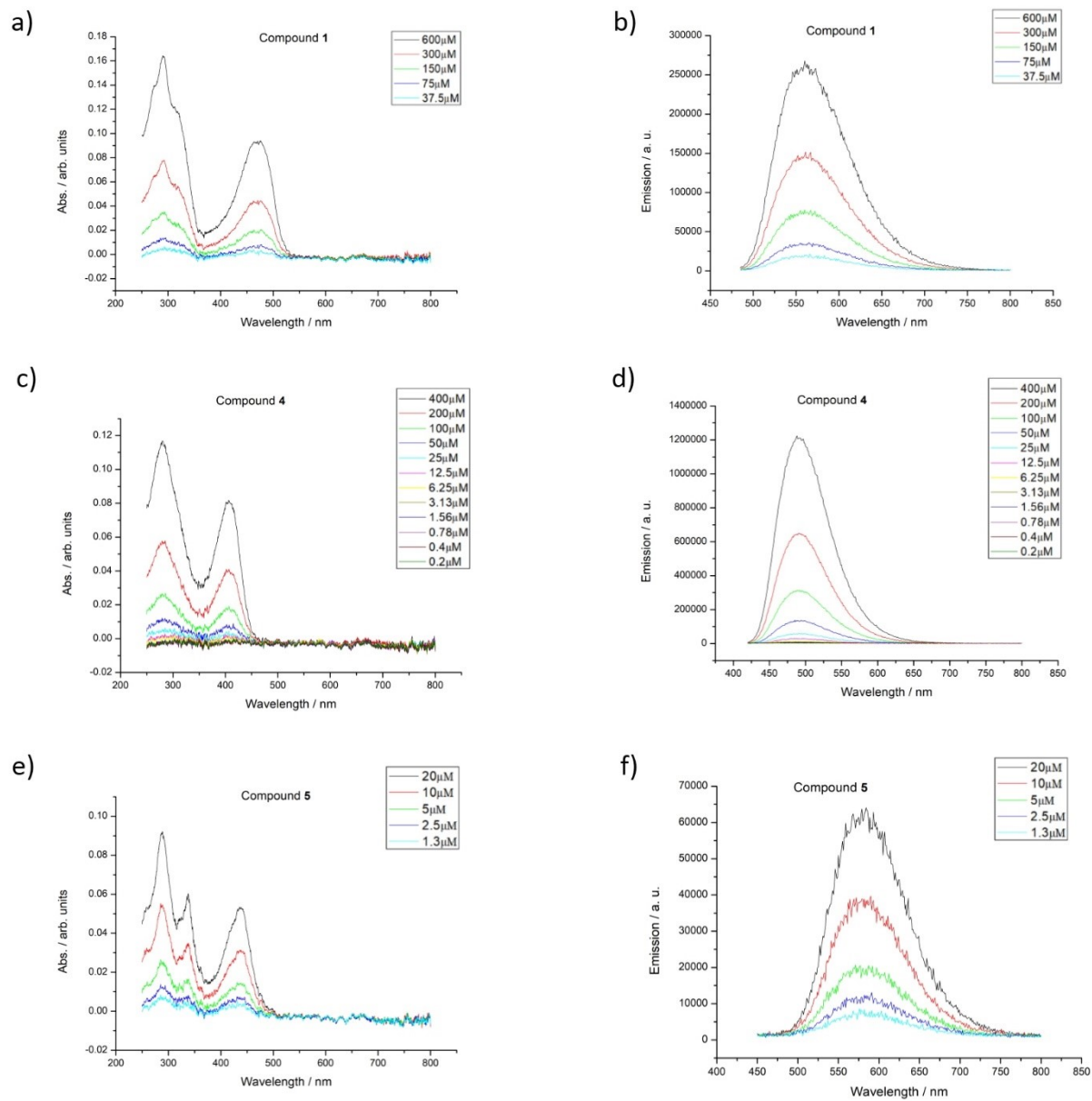
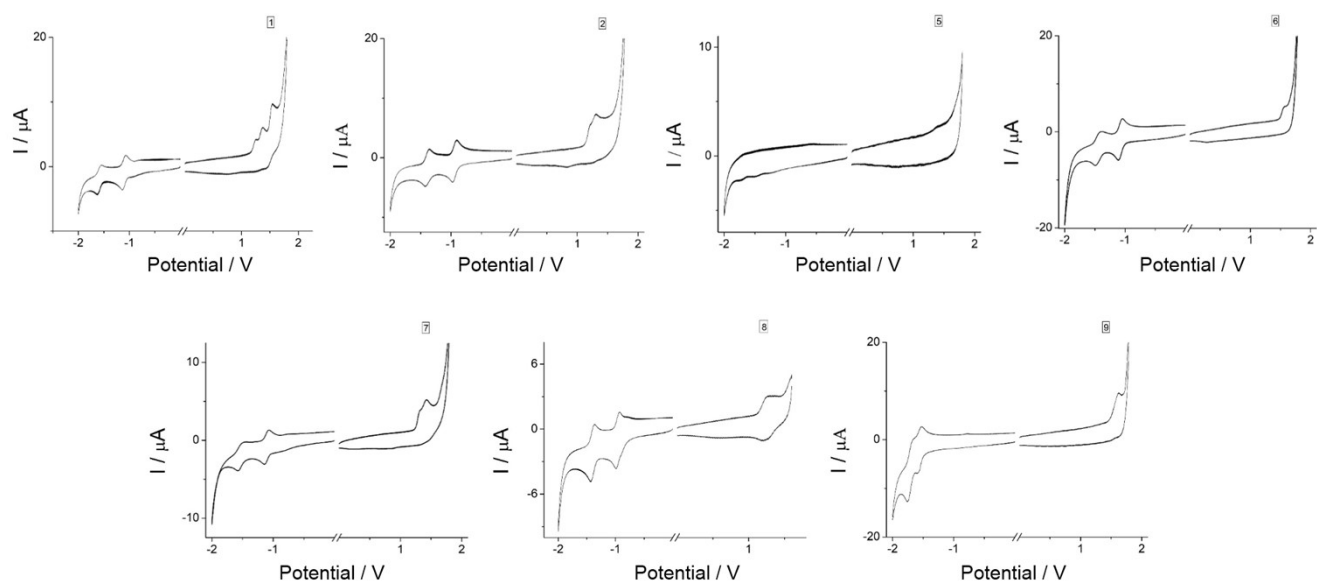


Figure S5. Concentration dependent absorption (a, c, e) and emission (b, d, f) spectra for LC compounds.





**Figure S6.** Cyclic voltammograms, measured in dichloromethane and scaled vs ferrocene potential.

**Table S4.** The  $E_{\text{red}}/E_{\text{ox}}$  are reduction and oxidation potentials in regard to ferrocene ( $\text{Fc}/\text{Fc}^+$ ) taken from cyclic voltammetry. The values of the formal potentials,  $E_{1/2}$ , obtained for each redox step in the voltammograms;  $E_{1/2}$  was approximated as  $(E_{\text{pa}} + E_{\text{pc}})/2$ , where  $E_{\text{pa}}$  and  $E_{\text{pc}}$  are the oxidation and reduction peak potentials, respectively.  $E_{\text{LUMO}}$  and  $E_{\text{HOMO}}$  are calculated energies of LUMO and HOMO levels, respectively.  $\Delta E$  is the energy gap between those levels.

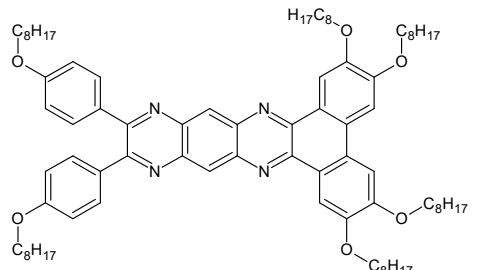
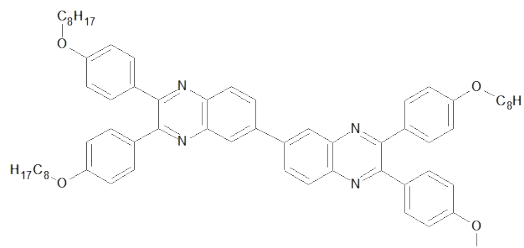
	$E_{\text{red}}$ [V]	$E_{\text{ox}}$ [V]	$E_{\text{LUMO}}$ [eV]	$E_{\text{HOMO}}$ [eV]	$\Delta E$ [eV]
<b>6</b>	-1.008	1.485	-3.307	-5.8	2.493
<b>7</b>	-1.053	1.248	-3.262	-5.563	2.301
<b>8</b>	-0.783	1.125	-3.532	-5.44	1.908
<b>9</b>	-1.489	1.47	-2.826	-5.785	2.959

**Table S5.** Collected electrochemical data compared to the spectral response of all compounds with their molecular structures;

No.	Formula	Abs. onset / nm, eV	Em. peak / nm, eV	$E_{\text{LUMO}}$ / eV	$E_{\text{HOMO}}$ / eV	$\Delta E_{\text{LUMO-HOMO}}$ / eV
<b>1</b>		520 2.38	560 2.21	-3,272	-5,495	2,223

## Supplementary Information

2		539 2.30	-	-3,454	-5,445	1,881
3		543 2.28	-	-	-	-
4		444 2.79	493 2.51	-2,841	-5,454	2,613
5		473 2.62	582 2.13	-2,961	-5,563	2,602
6		495 2.50	503 536 2.31	-3,307	-5,8	2,493
7		510 2.43	561 2.21	-3,262	-5,563	2,301

8		520 2.38	527 672 Weak 2.35 1.84	-3,532	-5,44	1,908
9		430 2,88	446 2,78	-2,826	-5,785	2,965

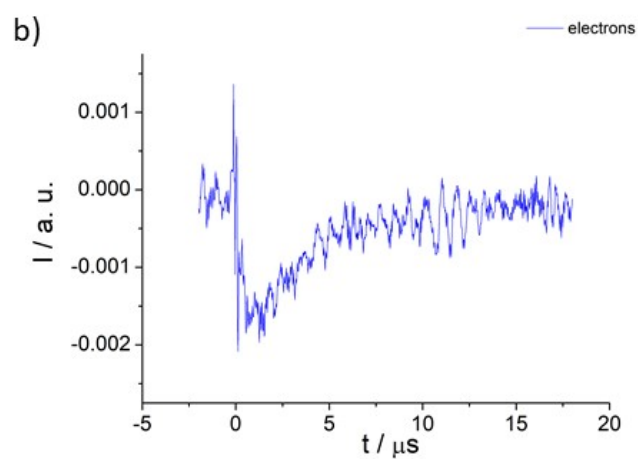
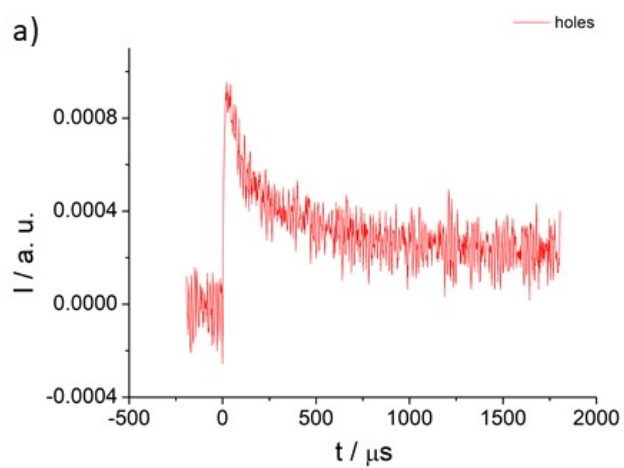
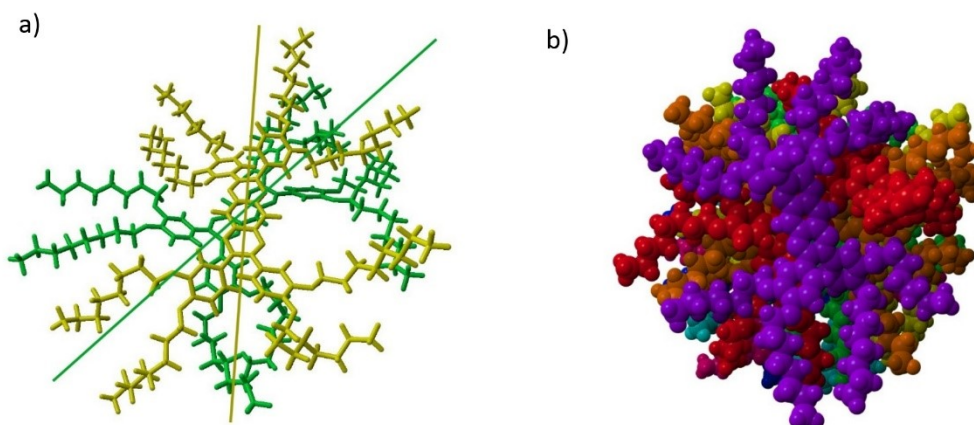


Figure S7. ToF results for compound 2; Green light (532 nm) excitation for holes (a) and electrons (b)



**Figure 58.** (a) Schematic drawing showing relative twist between neighbouring molecules in the column. (b) Projection along the column axis showing that the twist between neighbouring molecules results in uniform distribution of peripheral chains and assures good space-filling of the column stratum. Conformation of molecules in the aggregate was optimized using Force field Amber15IPQ implemented in YASARA software.

## References

1. C. J. Walsh and B. K. Mandal, *Chem Mater*, 2000, **12**, 287-289.
2. X. Wang, Y. Zhou, T. Lei, N. Hu, E. Q. Chen and J. A. Pei, *Chem Mater*, 2010, **22**, 3735-3745.
3. V. K. Vishwakarma, S. Nath, M. Gupta, D. K. Dubey, S. S. Swayamprabha, J. H. Jou, S. K. Pal and A. A. Sudhakar, *Acs Appl Electron Ma*, 2019, **1**, 1959-1969.
4. B. Mohr, V. Enkelmann and G. Wegner, *The Journal of Organic Chemistry*, 1994, **59**, 635-638.
5. P. Kizyckowska, A. Krówczyński, J. Kowalewska, J. Romiszewski, D. Pocięcha and J. Szydłowska, *Mol Cryst Liq Cryst*, 2012, **558**, 93-101.
6. C. Robinson, *Tetrahedron*, 1961, **13**, 219-234.